4462 *Chem. Mater.* **2009,** *21,* 4462–4467
DOI:10.1021/cm901073k

CHEMISTRY OF MATERIALS
Article

Nickel Phosphide Nanoparticles with Hollow, Solid, and Amorphous Structures

Junwei Wang, Aaron C. Johnston-Peck, and Joseph B. Tracy*

Department of Materials Science and Engineering, North Carolina State University, Raleigh, North Carolina 27695

Received April 18, 2009. Revised Manuscript Received August 14, 2009

Conversion of unary metal nanoparticles (NPs) upon exposure to oxygen, sulfur, selenium, and phophorus precursors usually produces hollow metal oxide, sulfide, selenide, or phosphide NPs through the Kirkendall effect. Here, nanostructural control of mixed-phase $Ni_2P/Ni_{12}P_5$ (represented as Ni_xP_y) NPs prepared through the thermolysis of nickel acetylacetonate using trioctylphosphine (TOP) as a ligand and phosphorus precursor is reported. The P:Ni molar ratio controls the NP size and is the key factor in determining the nanostructure. For P:Ni molar ratios of 1−3, nickel NPs form below 240 °C and subsequently convert to crystalline-hollow Ni_xP_y NPs at 300 °C. For higher P:Ni ratios, a Ni-TOP complex forms that requires higher temperatures for NP growth, thus favoring direct formation of Ni_xP_y rather than nickel. Consequently, for P:Ni molar ratios of >9, amorphous-solid Ni_xP_y NPs form at 240 °C and become crystalline-solid Ni_xP_y NPs at 300 °C. For intermediate P:Ni molar ratios of ∼6, both growth mechanisms result in a mixture of hollow and solid Ni_xP_y NPs. Similar results have been obtained using tributylphosphine or triphenylphosphine as the phosphorus source, but trioctylphosphine oxide cannot serve as a phosphorus source.

Introduction

Hollow nanoparticles (NPs) composed of metal oxides, sulfides, phosphides, and selenides, such as Co_xS_y,[1,2] Co_xSe_y,[1,3] CoO,[1,4] NiO,[5] and Ni_2P,[6−10] form when metal NPs react with suitable oxygen, sulfur, phosphorus, and selenium precursors. Core vacancies coalesce into a hollow void when core metal species diffuse outward faster than the oxygen-, sulfur-, phosphorus-, or selenium-containing species diffuse inward, which is known as the Kirkendall effect.[1,2,11] Control over porosity is important for many applications, including ion exchange, molecular separations, catalysis, and energy storage.[12] Notable examples are microporous zeolites,[13] mesoporous silicates,[14] and carbonaceous materials.[15]

Metal phosphides have been synthesized through the reduction of phosphates[16,17] and phosphinates,[18] solid-state metathesis at high temperatures,[19] low-temperature solvothermal methods,[20] and plasma methods.[21] Recently, trioctylphosphine (TOP)[7−10,17,22] and tris(trimethylsilyl)-phosphine[23] have been introduced as phosphorus reagents

*jbtracy@ncsu.edu.

(1) Yin, Y. D.; Rioux, R. M.; Erdonmez, C. K.; Hughes, S.; Somorjai, G. A.; Alivisatos, A. P. *Science* **2004**, *304*, 711–714.
(2) Yin, Y. D.; Erdonmez, C. K.; Cabot, A.; Hughes, S.; Alivisatos, A. P. *Adv. Funct. Mater.* **2006**, *16*, 1389–1399.
(3) Gao, J. H.; Zhang, B.; Zhang, X. X.; Xu, B. *Angew. Chem., Int. Ed.* **2006**, *45*, 1220–1223.
(4) Tracy, J. B.; Weiss, D. N.; Dinega, D. P.; Bawendi, M. G. *Phys. Rev. B* **2005**, *72*, 064404.
(5) (a) Nakamura, R.; Lee, J. G.; Mori, H.; Nakajima, H. *Philos. Mag.* **2008**, *88*, 257–264. (b) Nakamura, R.; Tokozakura, D.; Lee, J. G.; Mori, H.; Nakajima, H. *Acta Mater.* **2008**, *56*, 5276–5284. (c) Johnston-Peck, A. C.; Wang, J.; Tracy, J. B. *ACS Nano* **2009**, *3*, 1077–1084.
(6) Brock, S. L.; Perera, S. C.; Stamm, K. L. *Chem.—Eur. J.* **2004**, *10*, 3364–3371.
(7) Chiang, R. K.; Chiang, R. T. *Inorg. Chem.* **2007**, *46*, 369–371.
(8) Henkes, A. E.; Vasquez, Y.; Schaak, R. E. *J. Am. Chem. Soc.* **2007**, *129*, 1896–1897.
(9) Henkes, A. E.; Schaak, R. E. *Chem. Mater.* **2007**, *19*, 4234–4242.
(10) Senevirathne, K.; Burns, A. W.; Bussell, M. E.; Brock, S. L. *Adv. Funct. Mater.* **2007**, *17*, 3933–3939.
(11) (a) Fan, H. J.; Gösele, U.; Zacharias, M. *Small* **2007**, *3*, 1660–1671. (b) Lou, X. W.; Archer, L. A.; Yang, Z. C. *Adv. Mater.* **2008**, *20*, 3987–4019.
(12) (a) Zhao, D. Y.; Yang, P. D.; Huo, Q. S.; Chmelka, B. F.; Stucky, G. D. *Curr. Opin. Solid-State Mater. Sci.* **1998**, *3*, 111–121. (b) Johnson, S. A.; Ollivier, P. J.; Mallouk, T. E. *Science* **1999**, *283*, 963–965.
(13) Cundy, C. S.; Cox, P. A. *Chem. Rev.* **2003**, *103*, 663–701.
(14) Kresge, C. T.; Leonowicz, M. E.; Roth, W. J.; Vartuli, J. C.; Beck, J. S. *Nature* **1992**, *359*, 710–712.
(15) Wan, Y.; Yang, H. F.; Zhao, D. Y. *Acc. Chem. Res.* **2006**, *39*, 423–432.
(16) (a) Gopalakrishnan, J.; Pandey, S.; Rangan, K. K. *Chem. Mater.* **1997**, *9*, 2113–2116. (b) Stamm, K. L.; Gamo, J. C.; Liu, G. Y.; Brock, S. L. *J. Am. Chem. Soc.* **2003**, *125*, 4038–4039.
(17) Gregg, K. A.; Perera, S. C.; Lawes, G.; Shinozaki, S.; Brock, S. L. *Chem. Mater.* **2006**, *18*, 879–886.
(18) Guan, Q. X.; Li, W.; Zhang, M. H.; Tao, K. Y. *J. Catal.* **2009**, *263*, 1–3.
(19) Kleinke, H.; Franzen, H. F. *Angew. Chem., Int. Ed. Engl.* **1996**, *35*, 1934–1936.
(20) (a) Qian, X. F.; Xie, Y.; Qian, Y. T.; Zhang, X. M.; Wang, W. Z.; Yang, L. *Mater. Sci. Eng., B* **1997**, *49*, 135–137. (b) Barry, B. M.; Gillan, E. G. *Chem. Mater.* **2008**, *20*, 2618–2620.
(21) Wang, A. J.; Qin, M. L.; Guan, J.; Wang, L.; Guo, H. C.; Li, X.; Wang, Y.; Prins, R.; Hu, Y. K. *Angew. Chem., Int. Ed.* **2008**, *47*, 6052–6054.
(22) (a) Qian, C.; Kim, F.; Ma, L.; Tsui, F.; Yang, P. D.; Liu, J. *J. Am. Chem. Soc.* **2004**, *126*, 1195–1198. (b) Park, J.; Koo, B.; Yoon, K. Y.; Hwang, Y.; Kang, M.; Park, J. G.; Hyeon, T. *J. Am. Chem. Soc.* **2005**, *127*, 8433–8440.
(23) Perera, S. C.; Tsoi, G.; Wenger, L. E.; Brock, S. L. *J. Am. Chem. Soc.* **2003**, *125*, 13960–13961.

 Published on Web 09/16/2009

for the solution-phase synthesis of metal phosphide NPs. Several metals, including nickel, are thought to catalytically cleave C−P bonds in TOP, thus liberating phosphorus.[9,24] Ni_2P is an *n*-type semiconductor with a bulk band gap of 1.0 eV[25] with potential uses in solar cells[26] and catalysis.[6,10,18,27] The Schaak and Chiang groups have reported methods for preparing hollow Ni_2P NPs, with the chief focus on the conversion of nickel to Ni_2P NPs through a reaction with TOP.[7,8] They have also briefly reported solid Ni_2P NPs[10] and discussed possible reasons for its formation (rather than hollow cores), but the conditions for nanostructural control of Ni_2P NPs remain substantially unexplored.

Here, nanostructural control of mixed-phase Ni_2P/$Ni_{12}P_5$ (represented as Ni_xP_y) NPs prepared through the thermolysis of nickel acetylacetonate using TOP as a ligand and phosphorus precursor is reported. The P:Ni molar ratio controls the NP size and is the key factor in determining the nanostructure. For P:Ni molar ratios of 1−3, nickel NPs form below 240 °C and subsequently convert to crystalline-hollow Ni_xP_y NPs at 300 °C. For higher P:Ni molar ratios, a Ni-TOP complex forms that requires higher temperatures for NP growth, thus favoring direct formation of Ni_xP_y rather than nickel. Consequently, for P:Ni molar ratios of >9, amorphous-solid Ni_xP_y NPs form at 240 °C and become crystalline-solid Ni_xP_y NPs at 300 °C. For intermediate P:Ni molar ratios of ∼6, both growth mechanisms result in a mixture of hollow and solid Ni_xP_y NPs. Similar results have been obtained using tributylphosphine or triphenylphosphine as the phosphorus source, but trioctylphosphine oxide cannot serve as a phosphorus source. Nanostructural control of other metal oxide, sulfide, selenide, and phosphide NPs may also be possible by adjusting the reactant stoichiometry, which provides new opportunities to tune the physical properties of NPs.

Experimental Section

All NP syntheses were performed using standard airless procedures and commercially available reagents without further purification. Our synthetic methods are based on previously reported procedures.[7,8,28] Ni_xP_y NPs with different structures were prepared by adjusting a few parameters of a common thermal decomposition method: Except where noted otherwise, for each synthesis, 0.200 g (0.778 mmol) nickel acetylacetonate [$Ni(acac)_2$, 98%, TCI] and 2.0 mL (6.1 mmol) oleylamine (97%, Pfaltz & Bauer) were added to 5.0 mL (15.7 mmol) of 1-octadecene (ODE, 90%, Sigma−Aldrich) in a three-necked, round-bottomed flask. Upon heating to 80 °C while stirring, the solution became transparent. After degassing under vacuum at 80 °C for 2 h and backfilling with nitrogen, TOP (97%, Strem) of varying amounts was added by syringe. Different heating procedures were also used. For the two-step procedures, the reaction mixture was cooled to room temperature after initial heating and was then reheated after adding more TOP.

Two-Step Synthesis of Crystalline-Hollow Ni_xP_y Nanoparticles. Initially, 0.30 mL (0.67 mmol) of TOP was added by syringe at room temperature. Rapidly increasing the temperature to 240 °C (∼20 °C/min ramp rate) and maintaining this temperature for 30 min generated nickel NPs. For conversion to crystalline-hollow Ni_xP_y NPs, the flask was first cooled to room temperature. During the second step, an additional 4.70 mL (10.5 mmol) of TOP was added at room temperature, followed by rapid heating to 300 °C and aging for 30 min before cooling to room temperature.

One-Step Synthesis of Crystalline Ni_xP_y Nanoparticles. This procedure was the same as that used for the previously described two-step crystalline-hollow NPs, except 0.3−10.0 mL (0.7−22.4 mmol) of TOP was added initially, and then the temperature was rapidly increased to 300 °C for 30 min.

Two-Step Synthesis of Solid Ni_xP_y Nanoparticles. Initially, 3.00 mL (6.73 mmol) of TOP was added by syringe. After rapidly increasing the temperature to 240 °C for 30 min, the solution was cooled to room temperature. A small aliquot of the amorphous-solid Ni_xP_y NPs was removed, and the solution was reheated to 300 °C for another 30 min for conversion to crystalline-solid Ni_xP_y NPs.

Tributylphosphine and Triphenylphosphine. Ni_xP_y NPs were also synthesized using tributylphosphine (TBP) (97%, Sigma−Aldrich) or triphenylphosphine (TPP) (99%, Strem), instead of TOP. Crystalline-hollow Ni_xP_y NPs formed when heating 0.30 mL (1.2 mmol) of TBP in 5.0 mL of ODE or 0.20 g (0.76 mmol) of TPP in 5.0 g (13 mmol) of trioctylphosphine oxide (TOPO, 90%, Sigma−Aldrich) for 30 min at 300 °C. Crystalline-solid Ni_xP_y NPs formed when the amount of the phosphine was increased to 3.00 mL (12.0 mmol) of TBP in 5.0 mL of ODE or 1.00 g (3.81 mmol) of TPP in 5.0 g of TOPO. Solid, slightly aspherical Ni_xP_y NPs resulted when 5.0 g of TPP were heated at 240 °C for 30 min in 5.0 mL of ODE. Continued heating to 300 °C for 30 min drove further crystallization, accompanied by significant faceting.

Processing. After allowing each solution of NPs to cool to room temperature, methanol was added to flocculate the NPs, followed by centrifugation to separate the NPs from the solvent and excess ligands. The NPs were repeatedly (1−3 times) redispersed in hexanes, flocculated by adding methanol, and isolated by centrifugation. The NPs were stored dispersed in hexanes. Specimens for transmission electron microscopy (TEM) were prepared by placing a drop of NP solution from hexanes on an ultrathin, amorphous carbon and Formvar substrate and allowing the solvent to evaporate.

Transmission Electron Microscopy (TEM). The size and morphology of as-synthesized samples were measured by TEM and high-resolution transmission electron microscopy (HRTEM). Conventional bright-field imaging, selected-area electron (SAED), and energy-dispersive X-ray spectroscopy (EDS) were performed using a JEOL Model 2000FX microscope whose camera length was calibrated using aluminum. HRTEM imaging was conducted on a JEOL Model 2010F microscope.

Powder X-ray Diffraction (XRD). Nanoparticle powders deposited on silicon substrates were analyzed using a Bruker

(24) Chen, J. H.; Tai, M. F.; Chi, K. M. *J. Mater. Chem.* **2004**, *14*, 296–298.
(25) Panneerselvam, A.; Malik, M. A.; Afzaal, M.; O'Brien, P.; Helliwellt, M. *J. Am. Chem. Soc.* **2008**, *130*, 2420–2421.
(26) (a) Sharon, M.; Tamizhmani, G. *J. Mater. Sci.* **1986**, *21*, 2193–2201. (b) Sharon, M.; Tamizhmani, G.; Levyclement, C.; Rioux, J. *Sol. Cells* **1989**, *26*, 303–312.
(27) (a) Stinner, C.; Prins, R.; Weber, T. *J. Catal.* **2001**, *202*, 187–194. (b) Sawhill, S. J.; Phillips, D. C.; Bussell, M. E. *J. Catal.* **2003**, *215*, 208–219. (c) Oyama, S. T. *J. Catal.* **2003**, *216*, 343–352.
(28) Lee, I. S.; Lee, N.; Park, J.; Kim, B. H.; Yi, Y. W.; Kim, T.; Kim, T. K.; Lee, I. H.; Paik, S. R.; Hyeon, T. *J. Am. Chem. Soc.* **2006**, *128*, 10658–10659.

Table 1. Summary of Synthetic Conditions for Nanostructural Control of Ni_xP_y Nanoparticles

figure	synthetic conditions	nanostructure[a]
1a, 1d	0.30 mL of TOP, 240 °C for 30 min	CS (Ni)
1b, 1e	0.30 mL of TOP, 240 °C for 30 min, added 4.70 mL of TOP, then 300 °C for 30 min	CH
1c, 1f	5.00 mL of TOP, 300 °C for 30 min	CS
2a	0.30 mL of TOP, 300 °C for 30 min	CH
2b	0.50 mL of TOP, 300 °C for 30 min	CH
2c	1.00 mL of TOP, 300 °C for 30 min	CH
2d, 3a−c	2.00 mL of TOP, 300 °C for 30 min	CH/CS
3d	3.00 mL of TOP, 300 °C for 30 min	CS
3e, 3f	10.0 mL of TOP, 300 °C for 30 min	CS
4a−c	3.00 mL of TOP, 240 °C for 30 min	AS
4d−f	3.00 mL of TOP, 240 °C for 30 min, then 300 °C for 30 min	CS
6a	0.30 mL of TBP in 5.0 mL of ODE, 300 °C for 30 min	CH
6b	3.00 mL of TBP in 5.0 mL of ODE, 300 °C for 30 min	CS
6c	0.20 g of TPP in 5.0 g of TOPO, 300 °C for 30 min	CH
6d	1.00 g of TPP in 5.0 g of TOPO, 300 °C for 30 min	CS
6e	5.0 g of TPP in 5.0 mL of ODE, 240 °C for 30 min	AS/CS
6f	5.0 g of TPP in 5.0 mL of ODE, 240 °C for 30 min then 300 °C for 30 min	CS

[a] Abbreviations: CS: crystalline-solid; CH: crystalline-hollow; and AS: amorphous-solid. All compositions are Ni_xP_y, unless indicated otherwise.

D-5000 diffractometer (Cu K_α X-ray source) equipped with a Hi-Star area detector.

Results and Discussion

All NP syntheses applied a common approach: thermolysis of $Ni(acac)_2$ using oleylamine as a reducing agent and tertiary phosphines as both stabilizing ligands and phosphorus sources to form nickel or Ni_xP_y NPs. Oleylamine is known to serve as a reducing agent in the synthesis of metal[29] and metal oxide[30] NPs and is also presumed to reduce Ni(II) complexes to Ni(0) in this reaction. For every synthesis, all conditions were held constant except for the following parameters: (1) the amount of TOP (or, in a few instances, TBP or TPP) and the sequence of its addition, (2) the temperature ramp sequence, and (3) the solvent (usually ODE, but TOPO in a few cases). The results for each synthesis are summarized in Table 1.

Amount of TOP and the Temperature Ramp Sequence. Our first set of experiments showed that the P:Ni molar ratio is the critical parameter that determines whether crystalline-hollow or crystalline-solid NPs form (see Figure 1). In the two-step synthesis of crystalline-hollow Ni_xP_y NPs, nickel NPs (25 nm in diameter) were initially formed using 0.3 mL of TOP after heating at 240 °C for 30 min (see Figures 1a and 1d). Conversion of the nickel NP templates to Ni_xP_y was performed after cooling to room temperature and adding another 4.7 mL of TOP before heating to 300 °C for 30 min, which produced crystalline-hollow Ni_xP_y NPs (33 nm in total diameter; see Figures 1b and 1e and Figure S-1 in the Supporting Information). The rationale for cooling to room temperature before the second addition of TOP was to ensure separation between NP formation and conversion to Ni_xP_y. For comparison, in the one-step synthesis, the same total 5.0 mL volume of TOP was added in the first step, and the solution was directly heated to 300 °C for 30 min, which formed crystalline-solid Ni_xP_y NPs (8 nm; see Figures 1c and 1f). The remaining experiments give greater insight into the origin and details of the transition between hollow and solid Ni_xP_y NPs.

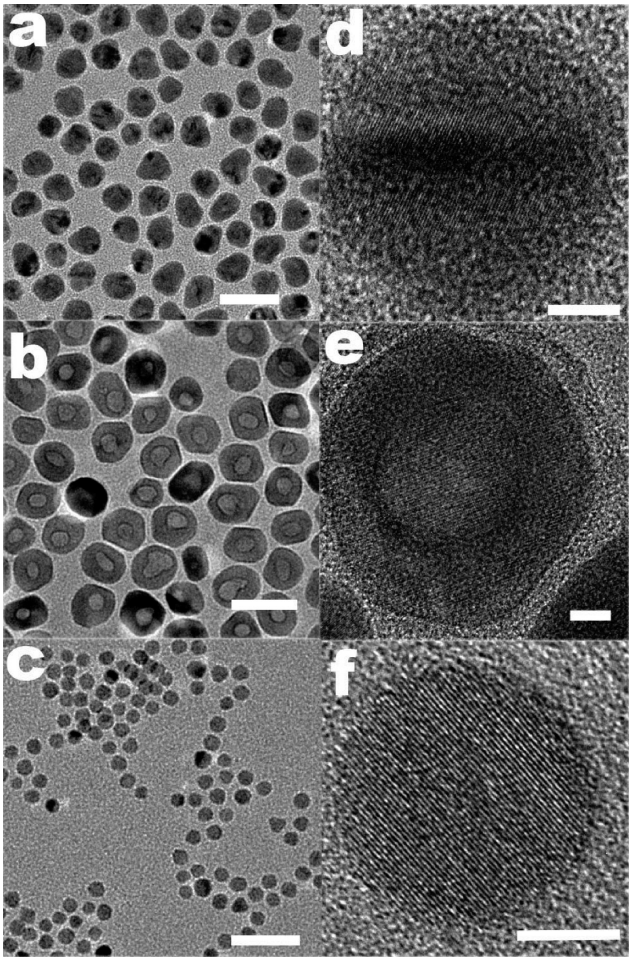

Figure 1. Transmission electron microscopy (TEM) images of crystalline NPs: (a,d) nickel NPs prepared at 240 °C using 0.30 mL of TOP; (b,e) hollow Ni_xP_y NPs formed from panel a via the two-step method after adding 4.70 mL of TOP and heating at 300 °C; (c,f) solid Ni_xP_y NPs synthesized using 5.00 mL of TOP after heating at 300 °C. Scale bars: (a−c) 50 nm, (d−f) 5 nm.

Significant structural and compositional changes accompany the conversion from crystalline nickel to crystalline-hollow Ni_xP_y NPs through the Kirkendall effect. Many of the nickel NPs are polycrystalline, as indicated by the differences in contrast over single NPs in Figure 1a. The crystalline-hollow Ni_xP_y NPs are usually single crystalline (see Figure 1b) and are more faceted than the nickel NPs from which they form, which indicates that the

(29) Hiramatsu, H.; Osterloh, F. E. *Chem. Mater.* **2004**, *16*, 2509–2511.
(30) (a) Nam, K. M.; Shim, J. H.; Ki, H.; Choi, S. I.; Lee, G.; Jang, J. K.; Jo, Y.; Jung, M. H.; Song, H.; Park, J. T. *Angew. Chem., Int. Ed.* **2008**, *47*, 9504–9508. (b) Xu, Z. C.; Shen, C. M.; Hou, Y. L.; Gao, H. J.; Sun, S. H. *Chem. Mater.* **2009**, *21*, 1778–1780.

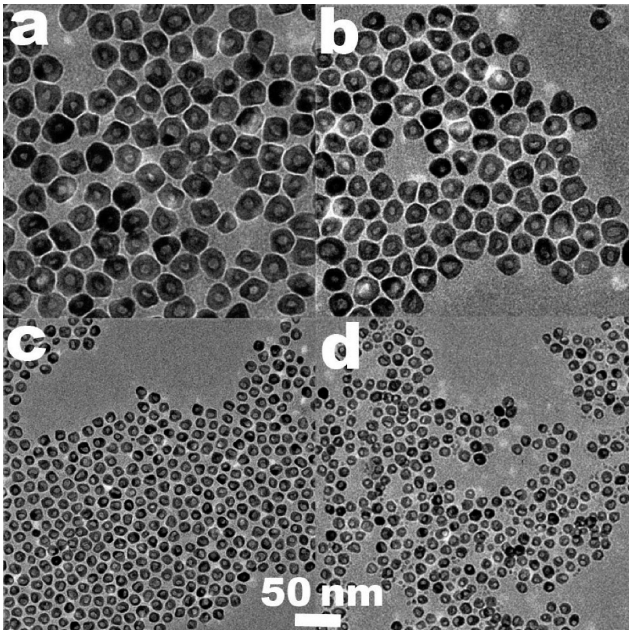

Figure 2. TEM images (same magnification) of crystalline Ni_xP_y NPs prepared following the one-step method after heating at 300 °C: hollow NPs produced using (a) 0.30 mL, (b) 0.50 mL, and (c) 1.00 mL of TOP; (d) mixture of hollow and solid NPs using 2.00 mL of TOP.

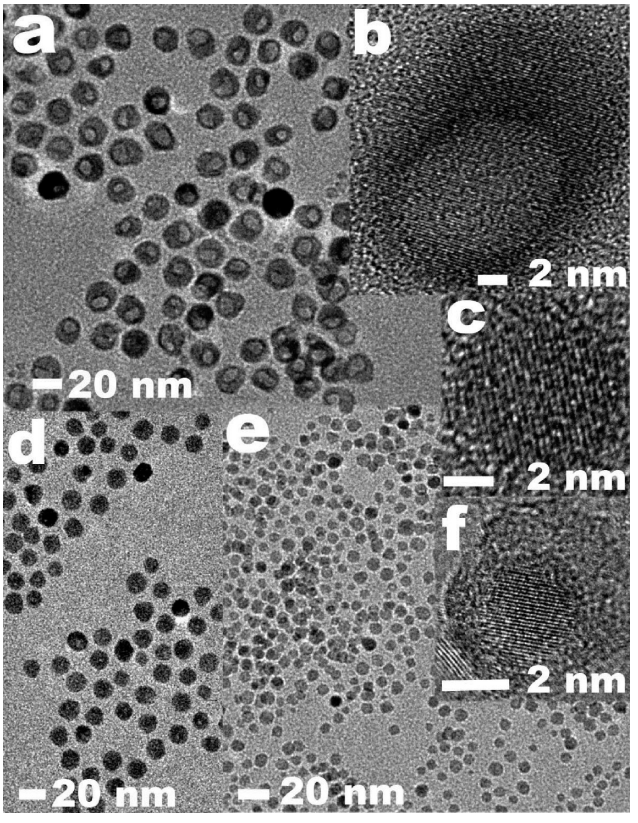

Figure 3. TEM and HRTEM images of crystalline Ni_xP_y NPs prepared following the one-step method after heating for 30 min at 300 °C: (a) mixture of hollow and solid NPs using 2.00 mL of TOP; (b,c) larger hollow and smaller solid Ni_xP_y NPs from panel a; (d) solid NPs prepared using 3.00 mL of TOP; (e,f) solid NPs prepared using 10.0 mL of TOP.

diffusion process also drives a change in the crystallinity. The product has a larger diameter, because of the volume of the core void and lattice expansion to form Ni_xP_y while

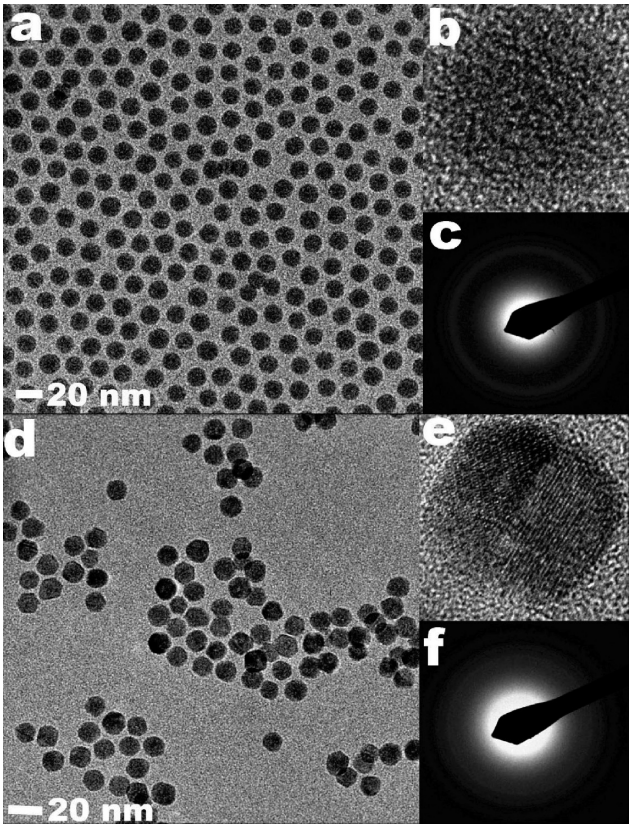

Figure 4. TEM, HRTEM, and SAED of the same batch of Ni_xP_y NPs prepared following the two-step method for solid NPs using 3.00 mL of TOP: (a−c) amorphous-solid, after heating at 240 °C for 30 min; (d−f) crystalline-solid, after subsequent heating at 300 °C for 30 min.

conserving the number of Ni atoms in each NP during the conversion. Several different nickel phosphide stoichiometries are known,[31] and our assignment as $Ni_2P/Ni_{12}P_5$ is based on powder X-ray diffraction (XRD) measurements (shown in Figure 5, presented later in this paper) and is further supported by SAED measurements (see Figure S-2 in the Supporting Information).

Transition from Hollow to Solid Nanoparticles. To gain an understanding of the role of the amount of TOP in controlling the NP growth, we performed several one-step syntheses using different amounts of TOP (0.3−10 mL) added to the flask initially, followed by a single fast temperature ramp to 300 °C for 30 min (see Figures 2 and 3). The use of 0.30 mL of TOP gave the same result as above in the two-step process, which implies that nickel NPs form at ∼200−240 °C during fast heating, followed by their conversion to Ni_xP_y at higher temperatures. The NP size decreases when larger amounts of TOP are used. *For 0.3−1.0 mL of TOP* (*P:Ni molar ratios of 0.9−2.8*), *the NP cores are consistently hollow*. A crossover behavior is observed for the sample using 2.0 mL of TOP (P:Ni molar ratio of 5.8) (see Figures 2d and 3a), which consists of two distinct, relatively monodisperse Ni_xP_y NP populations: larger (19 nm) crystalline-hollow NPs (see Figure 3b) and smaller (6 nm) crystalline-solid NPs (see Figure 3c). At lower temperatures, solid nickel NPs form

(31) Greenwood, N. N.; Earnshaw, A. *Chemistry of the Elements*, 2nd ed.; Butterworth-Heinemann: Boston, 1997; pp 489−492.

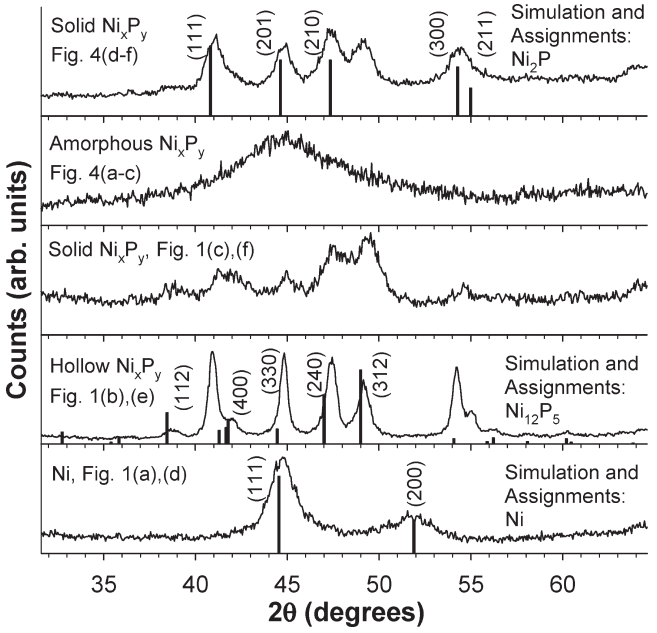

Figure 5. Powder X-ray diffraction (XRD) of selected nickel NPs and Ni_xP_y NPs. (All NPs are from the same batches whose TEM images are reported in Figures 1−4, except the nickel NPs, which are from another batch prepared according to the same procedure.)

first, followed by their conversion to crystalline-hollow Ni_xP_y at higher temperatures that occurs concurrently with the formation of crystalline-solid Ni_xP_y NPs. The size differences reflect differences in the growth behavior for these two populations. *Volumes of 3.0 mL TOP* (*P:Ni molar ratio of 8.6*) *and greater consistently produced smaller, crystalline-solid* Ni_xP_y *NPs* (see Figure 3d−f). HRTEM (Figure 3f and Figure S-3 in the Supporting Information) shows that the smaller, solid NPs contain single-crystal cores encapsulated in thicker amorphous shells when larger amounts of TOP are used.

TOP forms a molecular complex with nickel that inhibits the nucleation and growth of nickel NPs[22,32] and gives these two regimes of Ni_xP_y NP formation. Higher nucleation and growth temperatures are needed to decompose the Ni-TOP complex when larger amounts of TOP are used. The color of the reaction mixture before completing NP growth provides further evidence that the nucleation temperature is dependent on the amount of TOP: When 0.3 mL of TOP was used, the solution's color changed from green (color of reactants) to black at 200 °C, corresponding to the formation of nickel NPs. In contrast, when using 3.0 mL or more of TOP, the solution became and remained light brown at 230 °C, which indicates incomplete NP formation.

Amorphous- and Crystalline-Solid Nanoparticles. The two-step synthesis of solid Ni_xP_y NPs was a modification of the one-step method, in which the sample was temporarily cooled to room temperature after heating at 240 °C for 30 min for removal of an aliquot of solution. XRD, HRTEM, and SAED measurements of the aliquot for a synthesis using 3.0 mL of TOP show that the product is amorphous-solid Ni_xP_y NPs (see Figure 4a−c). *Subsequent heating to 300 °C for 30 min converts amorphous NPs to crystalline-solid, faceted* Ni_xP_y *NPs* (see Figure 4d−f). Energy-dispersive spectroscopy (EDS) analysis (see Figure S-4 in the Supporting Information) shows that the P:Ni molar ratios in the amorphous aliquot and the crystalline product are almost the same. The compositions of the crystalline phases are known and can be used as a reference for the composition of the amorphous NPs. The compositions of the amorphous and crystalline NPs could be slightly different, however, because EDS measurements have limited precision, and there could also be small differences in the amounts of residual TOP in each sample. A control sample of the TOP-stabilized Ni NPs was also analyzed, which had considerably less phosphorus content, as expected. Crystallization of the amorphous NPs involves primarily or exclusively short-range diffusion, because the composition either does not change or changes minimally during the reaction. If the composition of the amorphous NPs had been nickel or had been significantly deficient in phosphorus, then the conversion to hollow Ni_xP_y would likely occur through the Kirkendall effect. Crystallization is often associated with faceting,[33] and a similar annealing process is known to convert poorly crystallized face-centered cubic (fcc) (almost amorphous) cobalt NPs to a crystalline hexagonal close-packed (hcp) phase.[34]

Structural Analysis. The previously discussed structures were confirmed via powder XRD (see Figure 5). All of the crystalline nickel phosphide samples have distinct Ni_2P and $Ni_{12}P_5$ phases, which were also observed in SAED measurements (see Figure S-2 in the Supporting Information). In comparison with other reports of pure[8] and less-pure[7] Ni_2P phases, $Ni_{12}P_5$ might form under milder conditions, whereas the conversion to pure Ni_2P could require prolonged growth times or higher temperatures[9,10] than those reported here.

Implications. A minimum size of nickel NP required for conversion to hollow Ni_xP_y through the Kirkendall effect has not been proven but is plausible,[8] because the decreased radius of curvature for smaller NPs favors inward diffusion of phosphorus and slows the outward diffusion of nickel. Our results do not directly address the issue of a minimum size: In this study, the composition (nickel or Ni_xP_y) at the start of NP growth determines whether conversion to a hollow structure is possible. Chiang's recent report of Ni_2P NPs includes TEM images of hollow Ni_2P NPs as small as 3−4 nm in total diameter.[7] Therefore, if there is a minimum size for conversion of solid nickel to hollow Ni_xP_y NPs, it is smaller than 3−4 nm.

Role of Trioctylphosphine Oxide. Several other studies have used trioctylphosphine oxide (TOPO) in combination with TOP for growing phosphide NPs.[7−9,17,22] We have also explored the role of TOPO and have found that

(32) Carenco, S.; Resa, I.; Le Goff, X.; Le Floch, P.; Mézailles, N. *Chem. Commun.* **2008**, 2568–2570.
(33) Yin, Y. D.; Erdonmez, C.; Aloni, S.; Alivisatos, A. P. *J. Am. Chem. Soc.* **2006**, *128*, 12671–12673.
(34) Lisiecki, I.; Salzemann, C.; Parker, D.; Albouy, P. A.; Pileni, M. P. *J. Phys. Chem. C* **2007**, *111*, 12625–12631.

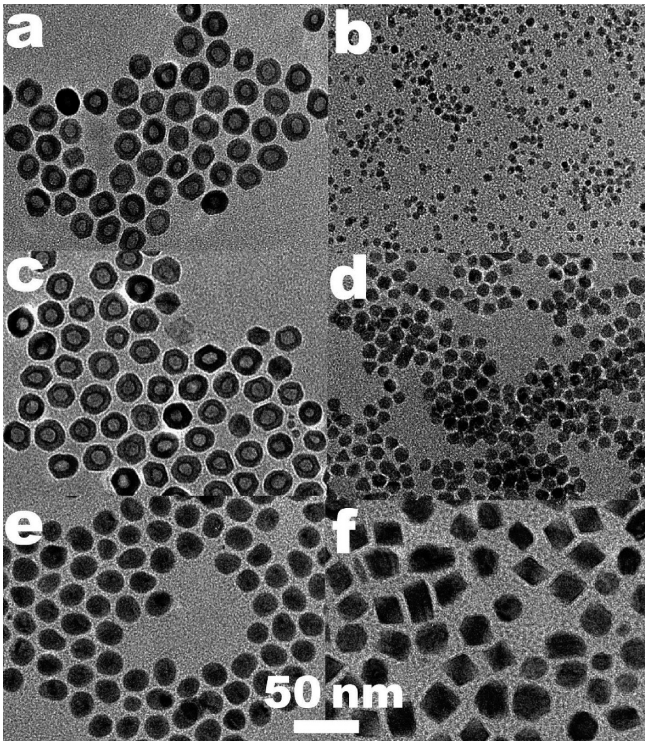

Figure 6. TEM images (same magnification) of Ni_xP_y NPs: (a,c) crystalline-hollow and (b,d) crystalline-solid NPs synthesized using (a) 0.30 mL of TBP or (b) 3.00 mL of TBP in 5.0 mL of ODE heated at 300 °C for 30 min, or (c) 0.20 g of TPP or (d) 1.00 g of TPP in 5.0 g of TOPO. The use of 5.0 g of TPP in 5.0 mL of ODE produced (e) partially crystalline-solid Ni_xP_y NPs after heating at 240 °C for 30 min that (f) more completely crystallized and became faceted upon heating to 300 °C for 30 min.

TOPO does not serve as a phosphorus precursor for growing Ni_xP_y NPs. TEM and SAED of the products from a synthesis using no TOP and 5.0 g of TOPO as the solvent (instead of ODE) show large nickel NPs (see Figure S-5 in the Supporting Information).

We have also repeated some of the above experiments with varying amounts of TOP while using TOPO as the solvent instead of ODE (see Figure S-6 in the Supporting Information). The same two regimes of hollow and solid NP growth were observed, but larger amorphous-solid Ni_xP_y NPs could be obtained using TOPO instead of ODE, which suggests that the transition between growth regimes is dependent on the solvent. When attempting to prepare crystalline-solid Ni_xP_y NPs by heating the reaction mixture to 300 °C, the NPs became insoluble, but the conversion could likely be conducted by first purifying the amorphous-solid Ni_xP_y NPs and redispersing them in another solvent. Generally, the solubility of nickel and Ni_xP_y NPs is better in TOPO than in ODE, and we recommend using TOPO as the solvent for future studies.

Use of Tributylphosphine and Triphenylphosphine. TBP and TPP are also suitable precursors for synthesizing hollow and solid Ni_xP_y NPs (see Figure 6). When a large amount of TPP was used for heating at 240 °C for 30 min, solid Ni_xP_y NPs formed that were at least partially crystalline and might also be partially amorphous. Upon further heating to 300 °C for 30 min, the same batch of NPs remained solid and became highly faceted, which is consistent with crystallization. The same general trend as

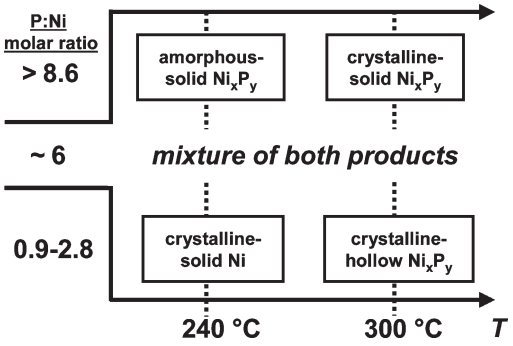

Figure 7. Summary of synthetic conditions for synthesizing nickel and Ni_xP_y NPs with different nanostructures.

that for TOP holds, in that small amounts produce crystalline-hollow structures and larger amounts give solid structures. Differences in the decomposition behavior and the NP sizes and structures resulting for a given molar amount of each phosphine are also expected, because each phosphine has distinct steric[35] and electronic properties. For quantitative control of the NP size and nanostructure, the reaction conditions must be established empirically for each tertiary phosphine and solvent combination.

Conclusions

Synthetic conditions for the nanostructural control of Ni_xP_y NPs are summarized in Figure 7. The P:Ni molar ratio determines whether the first NPs formed during the reaction are solid nickel or Ni_xP_y. Nickel-template NPs are converted to hollow Ni_xP_y NPs at higher temperatures through the Kirkendall effect. The solid Ni_xP_y NPs initially form with amorphous structures, but they become crystalline upon annealing at 300 °C while remaining solid, because the diffusion is short-range. Although the molar ratios, temperatures, and concentrations used in this study are specific to the nickel−phosphorus system, the methods used to control the nanostructure of Ni_xP_y NPs can likely be adapted to provide nanostructure-controlled growth of other metal oxide, sulfide, selenide, and phosphide NPs.

Acknowledgment. This work was supported by an NSF NER grant (No. EECS-0707315) and startup funds from North Carolina State University. We thank Jon-Paul Maria for the XRD measurements and Tom Rawdanowicz and Trinity Biggerstaff for the TEM training.

Note Added after ASAP Publication. There was an error in the first column of Table 1 in the version published ASAP September 16, 2009; the corrected version was published ASAP September 17, 2009.

Supporting Information Available: Additional TEM, HRTEM, and SAED measurements for selected samples, EDS analysis of solid NP samples, synthesis of Ni NPs in TOPO without TOP, and synthesis of Ni_xP_y NPs in TOPO rather than ODE. (PDF) This material is available free of charge via the Internet at http://pubs.acs.org.

(35) Tolman, C. A. *Chem. Rev.* **1977**, *77*, 313–348.